ASSESSING THE FATIGUE RESPONSE OF GLASS FIBER REINFORCED SUSTAINABLE POLYMER MATRIX COMPOSITES

Jayaram R. Pothnis[1], Akshay Hejjaji[1], Gursahib S. Bhatia[1], Salwa Sandali[1] and Anthony J. Comer[1]

[1] Bernal Institute, School of Engineering, University of Limerick, Limerick V94 T9PX, Ireland, Jayaram.Pothnis@ul.ie, https://bernalinstitute.com

Keywords: Infusible Thermoplastic, Bio-based Thermoset, Fatigue Response

ABSTRACT

Rapid climate change has necessitated the need for finding clean and green sources of energy. The offshore wind and tidal energy sector has found increasing relevance in this regard. Polymer composites can be functionally viable materials while offering distinct advantages such as high specific mechanical properties and better corrosion resistance over traditional materials such as steel, which are widely employed at present in the construction of offshore energy structures. However, inadequate material characterization data under various loading conditions, especially fatigue is hindering their large-scale utilization for offshore structural applications. The EU-funded FIBREGY project is aimed at addressing this material characterization inadequacy to increase the use of composites in offshore structures while reducing their environmental impact. In this paper, the fatigue behavior of unidirectional glass fiber composites under tension-tension loading is presented. A bio-based thermoset epoxy resin and an infusible thermoplastic resin were the matrix materials for the composites. The composites were tested in a direction transverse to the fiber axis. In addition to the conventional S-N curve method to determine fatigue life, the thermography technique was employed to assess the fatigue behavior of the composites. The behavior of the composites with thermoset and thermoplastic matrix materials were compared and the results are included. The fatigue limit of composites with the thermoplastic matrix was over 20 % lower as compared to that of composites with thermoset matrix. Further, the failure mechanisms and fracture characteristics of the composites were studied by examining the fracture surfaces of failed specimens using Scanning Electron Microscopy technique. The observations are discussed in the context of the fatigue test results.

1 INTRODUCTION

In recent decades, climate change has led to significant environmental and economic consequences. To mitigate the effects of climate change, the power sector has been identified as one of the major areas that can contribute to reduction in pollution and with that the carbon footprint on the environment [1]. Further, this requirement is immediate to reduce climate-related impact. Within the power sector, wind energy has emerged as one of the major sources for the generation of renewable and clean energy. It has been recognized as virtually a pollution-free and carbon-free source of energy [2, 3]. Subscribing to this observation, the wind energy industry has grown consistently in the past few decades with the global cumulative capacity increasing over four times between 2009 and 2019 itself reaching 651 GW of capacity globally [4]. While initial development of wind energy was through the development of onshore wind farms, offshore wind and tidal energy systems are increasingly being installed world over and continue to grow [5, 6].

From the materials perspective, presently conventional materials such as steel have been largely employed for the construction of offshore energy structures. Given the harsh and corrosive marine environment, the structures exhibit poor resistance to corrosion driving up installation and maintenance costs. Polymer composites are seen to meet the functional requirements of these offshore structures while reducing the costs required for maintenance [7]. However, at present the mechanical behavior of these composites, especially their fatigue response is yet to be completely understood and hence, hindering their large-scale application in offshore energy structures. The Horizon 2020 EU-funded

FIBREGY project (grant no. 952966) aims to address this aspect to facilitate extensive use of polymer composites for structural applications in offshore energy installations. Further, the end-of-life management of polymer composites has been a challenging aspect and adversely affecting the environment [8, 9]. Therefore, the project is also promoting the development of sustainable composites to reduce environmental footprint and increase recyclability.

During their service life, offshore structures are exposed to extreme environmental conditions including large temperature variations, gusts, rain, salinity etc. [10]. Structures are expected to withstand dynamic loading conditions during operation and hence a thorough understanding of the fatigue response of materials is required for the design process. Recognising this need, research efforts have focused on evaluating the fatigue properties of polymer composites comprising of a variety of fiber-matrix combinations. Recently, Bakkal et al. [11] investigated the fatigue behavior of glass fiber/acrylic resin (elium) composites with different fiber orientations. The authors reported that the cross-ply laminates (0°/90°) exhibited the highest fatigue strength while the ±45° laminates recording the lowest strength. Stiffness degradation was higher in laminates with more off-axis plies in the stacking sequence. Another study evaluated the influence of seawater on the fatigue behavior of glass fiber composites with acrylic and epoxy matrix systems. They reported that the loss in cyclic properties of composites with acrylic matrix was lower as compared to that of the epoxy matrix composites due to seawater influx [12]. The fatigue behavior under tensile loading of flax/epoxy and glass/epoxy composites were compared by Liang et al. [13]. The authors observed that while fatigue endurance of glass/epoxy composites was higher in case of cross-ply laminates, it was lower as compared to that of flax/epoxy composites in case of off-axis specimens. In a study reported by Makeev [14], the interlaminar shear properties of glass and carbon fiber composites under fatigue loading was evaluated to understand onset of delamination failure in composite structures.

The works of Roundi et al. [15] and Mahboob et al. [16] are other recent studies focusing on understanding the fatigue performance of glass/epoxy composites. Since characterizing fatigue behavior is complex, time consuming and expensive, the data available in open literature is still limited and further evaluation of material fatigue behavior is required. The focus of this paper on characterizing and comparing the fatigue behavior of glass fiber composites fabricated using two different sustainable matrix systems. Two polymers namely a bio-based epoxy resin and an infusible thermoplastic acrylic resin were chosen as the matrix materials to manufacture unidirectional (UD) glass fiber (GF) composites. The tension-tension fatigue behavior of the specimens was characterized in the study. During testing, the specimens were loaded in a direction transverse to the fiber axis (90° configuration). This specimen configuration was chosen to understand the influence of the matrix type on the overall fatigue behavior of the composites. The classical S-N curve approach was used to evaluate the fatigue behavior. Additionally, thermography technique was also employed to evaluate the fatigue strength of the composites. In this technique, the heat generated during fatigue loading due to damage accumulation is monitored and the fatigue limit is estimated using a rapid temperature stabilization method [17]. Fatigue-induced damage is quantified based on the heat and energy data obtained during testing. Extensometer, strain gauges and acoustic emission sensors were also part of the instrumentation used during testing. The results of the fatigue testing are discussed in this paper.

2 MATERIALS AND METHODS

2.1 Materials

Unidirectional (UD) glass fiber composites were fabricated for the experimental studies using two different matrix systems. Non-crimp fabric of areal density 320 gsm (supplied by Gerster GmbH and Co. KG, Germany) was the reinforcement. The UD fibers were held in position by polyester fibers running in the weft direction. Elium resin (supplied by Arkema, France) was the thermoplastic matrix used along with Perkadox GB-50X powder as the cure initiator. The mix ratio of the Elium resin and cure initiator was 100:3 by weight. The bio-epoxy Infugreen resin with SD 8824 hardener (supplied by Sicomin, France) was the other matrix system employed to fabricate the composites. For this matrix system, a resin to hardener ratio of 100:22 by weight was used. The choice of matrix systems was based on their processability at ambient temperature, which can enable the fabrication of large-scale structures typically seen in the case of offshore structures. Further, the matrix systems were chosen based on their

sustainability credentials and the potential to be recycled in the case of the thermoplastic.

2.2 Manufacture of specimens

Two UD glass fiber (GF) reinforced laminates, one each using the two different matrix systems were fabricated for the experimental work. The lay-up configuration was made up of 18 layers of reinforcement and vacuum assisted resin infusion moulding was used for laminate fabrication. Figure 1 depicts the laminate fabrication process. The dry reinforcement fabric, peel ply release film and flow medium were placed in the appropriate order on a glass moulding plate. This arrangement was then enclosed in a vacuum bag, which in turn was secured to the glass plate using sealant tape. With the resin inlet and air exit tubes in position, the complete arrangement was checked for leaks using a vacuum pump. During infusion, a pressure of 10–20 mbar (absolute) was maintained inside the vacuum bag and the resin was infused at ambient temperature. A similar process was followed to fabricate laminates using the two different resin systems. Laminates of thickness 4±0.1 mm were fabricated and individual specimens of nominal gauge length 150 mm and width 25 mm were machined along the desired orientation using abrasive waterjet machining process. The specimens were post-cured subsequently in a hot air oven. While specimens fabricated using the thermoset resin were post-cured at 60°C for 16 hours, specimens fabricated using the thermoplastic resin were post-cured at the same temperature for 24 hours. The post-cure durations were as per manufacturer specifications.

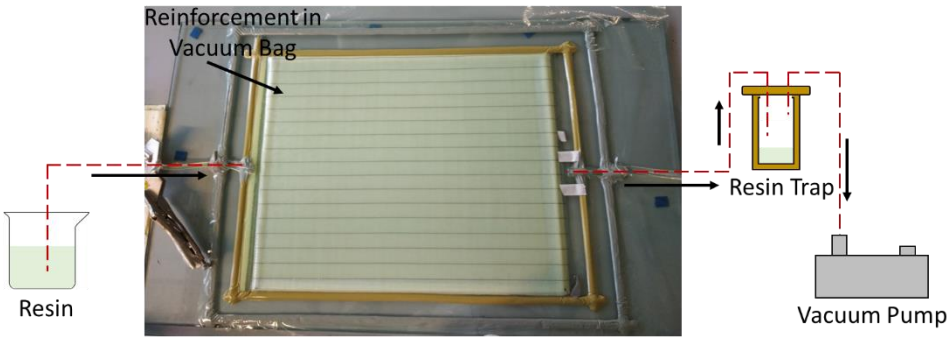

Figure 1: Vacuum assisted resin infusion process for fabricating laminates.

2.3 S-N curve testing

The fatigue limit of the glass fiber composites was evaluated using the S-N curve method. The tests were conducted in accordance with ISO 13003:2003 test standard [18]. The specimen geometry was based on the test coupon details outlined in ISO 527-4:2009 standard [19]. Accordingly, specimen gauge length was 150 mm and width 25 mm. The fatigue tests were performed on a Zwick servo-hydraulic test machine. A 100 kN load cell was employed on the machine for the tests. Quasi-static tensile tests were also performed on the same machine to establish the load levels required for the fatigue tests. These tests were conducted under displacement-controlled conditions of 1.5 mm/min. The constant amplitude tension-tension fatigue tests were performed maintaining a R ratio of 0.1. The fiber orientation in the specimens was perpendicular to the direction of loading (90° configuration). The specimens were tested at different cyclic stress levels at a frequency of 8 Hz to generate the S-N curves for determining the fatigue strength. During the tests, strain gage, acoustic emission sensor and an extensometer were mounted on the specimens to enable data acquisition. Figure 2 presents the experimental set-up used for fatigue testing.

2.4 Thermography tests

In addition to the S-N curve approach to determining the fatigue limit, temperature stabilization method was also used to estimate the fatigue stress level of the composites. The method is based on monitoring the change in specimen surface temperature during fatigue testing. This method is based on

the principle that the energy required to initiate damage is transformed into heat irreversibly and hence specimen damage or deformation is followed by an increase in temperature, which is monitored during testing. The change in specimen temperature during testing is recorded using an infrared (IR) camera. The change in temperature with increasing cyclic stress levels is recorded. The specimens are loaded for a pre-determined number of cycles at every stress level to allow for temperature to stabilize. This process is repeated at different stress levels, which are increased in a step-wise manner. The applied stress levels are based on the quasi-static tensile strength of the specimens. The change in temperature with stress levels is recorded and plotted. The required stress level is obtained as the intersection of two straight lines of different slopes that can be fitted using this data. This is referred to as the temperature stabilization method [17].

The load-controlled step-wise tests were performed on the same testing machine described earlier. In addition to the instrumentation used for the S-N curve tests, an IR camera was used in the experimental set-up to record specimen temperature during the tests. A Micro Epsilon TIM VGA thermal imager with a 33° lens was used to capture specimen temperature data. The specimens were subjected to fatigue loading starting at a stress level equal to 10 % of the quasi-static tensile strength. The stress level was gradually increased in steps of 5 % after every 8000 cycles of loading. These tests were performed at 10 Hz frequency at ambient temperature. Each step loading segment was separated by a dwell time of approximately 10 minutes to allow the specimens to return to ambient temperature. The thermal data was analysed subsequently to determine the specimen fatigue limit subsequently.

2.5 Fractography using scanning electron microscopy (SEM)

To gain insight about failure initiation and mechanisms of failure during fatigue testing, the fracture surfaces of failed specimens were examined using a Hitachi SU-70 high-resolution SEM instrument. Sections of specimens including the fracture surfaces were extracted from the failed specimens carefully for the analysis. These specimen sections were mounted onto specimen holders and the fracture surfaces were sputter coated with gold using an Emitech K550 sputter coater. The specimen sections were subsequently examined using SEM.

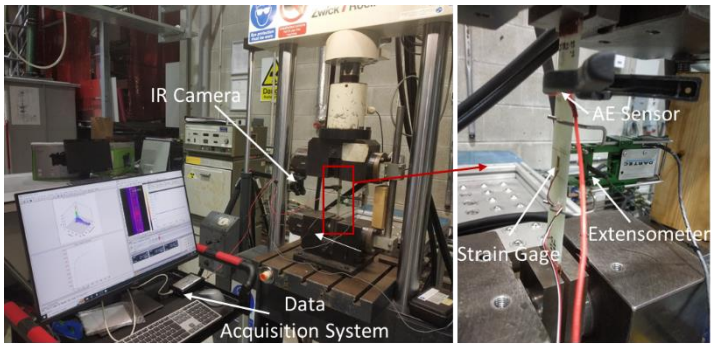

Figure 2: Experimental set-up for fatigue testing.

3 RESULTS AND DISCUSSION

The fatigue properties of GF/thermoplastic and GF/bio-epoxy composites were evaluated in the study. The fatigue properties were evaluated using two methods. The classic S-N curve and thermography methods. The results obtained from the tests are briefly discussed.

3.1 S-N curve testing

Figure 3 presents the results of the fatigue tests performed using S-N curve approach. For comparison, the S-N curves of both composites tested are included in the same figure. The S-N curves were obtained by testing the specimens with their fiber axis in a direction perpendicular to that of loading. The fatigue tests were performed at a frequency of 8 Hz maintaining a R ratio of 0.1. Quasi-

static tensile tests were performed earlier. The results of these tests are also included in Figure 3 for reference. The nominal quasi-static tensile strength value of GF/thermoplastic composites (90° configuration) was 38.8 MPa and the same in case of GF/bio-epoxy composites was 49.9 MPa. The stress levels for the fatigue tests were determined based on these quasi-static strength values. Figure 3 indicates the variation of maximum stress value with respect to the number of cycles of loading. It was observed that the stress values in case of composites with the bio-epoxy matrix was marginally higher as compared to that of composites with the thermoplastic matrix. Considering that specimen failure is matrix dominant in this configuration, the difference in matrix-fiber interfacial interaction is seen to play an important role in the observed results. Overall, the composite with bio-epoxy matrix is seen to exhibit better fatigue behavior as compared to the other composite. To further understand the difference in fatigue behavior between the two matrix types, the fracture surfaces of failed specimens were analysed and the findings are discussed in Section 3.3.

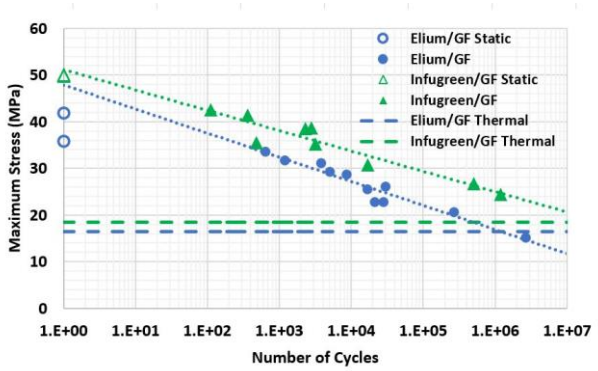

Figure 3: Fatigue test results of the composites obtained through S-N curve and thermography methods.

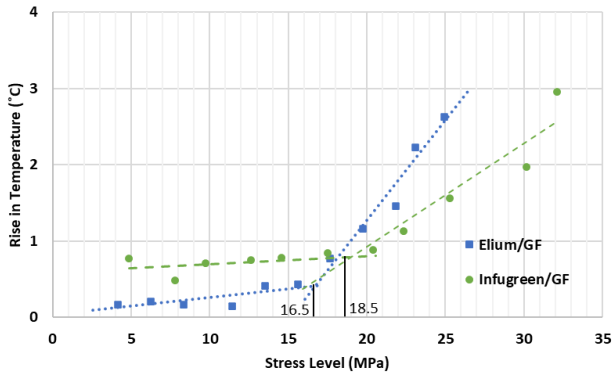

Figure 4: Change in specimen temperature at the end of each loading segment with applied stress for the composites tested.

3.2 Thermography tests

In addition to obtaining the fatigue limit values of the tested composites using S-N curve approach, preliminary tests were performed using the temperature stabilization method to obtain the threshold stress level of the composites. This method enables the determination of the threshold stress value quickly and efficiently in comparison with the S-N curve approach. The specimens were tested as per the procedure briefly described in Section 2.3. The preliminary test results of this method are included in Figure 3. With further testing and increasing number of tested specimens, a range of threshold stress values is expected to be obtained and the results will be updated. The variation of temperature with the applied stress level for the two types of composites is presented in Figure 4. It was observed that the change in temperature during a loading step increased with increasing applied stress level. A similar

trend was seen in both the types of composites tested. The initiation of damage and its subsequent increase is manifest in the form of temperature changes during the loading process. During the initial load steps, the increase in temperature was less indicating that the damage was insignificant during the initial stages of loading. Further, the temperature change during the initial stages was lesser in case of the composites with thermoplastic matrix. This can be observed in Figure 4. The temperature increase subsequently indicates damage progression ultimately leading to specimen failure. From the data of the change in temperature with applied stress, linear line segments were fitted. The data point sets in case of each composite were fitted into two different linear trend lines as seen in Figure 4. The stress level at the intersection of these two lines is then determined. In case of GF/bio-epoxy composite, the stress level at the intersection of the linear line segments was determined to be ≈ 18.5 MPa and in case of GF/thermoplastic composite, the value was ≈ 16.5 MPa. Beyond these stress values, damage accumulation and progression can be considered to increase as compared to the damage initiation and accumulation at lower stress levels. The trend in values was similar to that obtained using the S-N curve approach. Further, the difference in stress values obtained from thermography and S-N curve approaches was less as seen in Figure 3. The values indicate that thermography method can be employed to get an initial estimate of the threshold stress value of the composites quickly in a time efficient manner. For a detailed assessment, the S-N curve approach is required.

3.3 Fractography using scanning electron microscopy (SEM)

Specimens tested under fatigue loading were analysed using SEM. Based on the S-N curve data of the two types of composites tested, representative specimens from low cycle and high cycle fatigue regimes were chosen in each case for the analysis. Figure 5 (a) presents the typical GF/thermoplastic specimens tested under low and high cycle fatigue regimes. The location of final failure is indicated in Figure 5(a). Specimen failure was observed within the gauge length as seen. Failure was localized with evidence of fiber-matrix debonding and delamination seen at the location of failure. Figure 5(b) provides cross-sectional information of specimens prior to fatigue testing. The images indicate the presence of polyester construction fibers along with the glass fibers. In some locations, the construction fibers were observed to be grouped, possibly displaced by the evolving resin flow front during laminate fabrication. This displacement of construction fibers leads to an uneven distribution of resin-rich segments within the composite. Figures 5(c) and 5(d) present the SEM images drawn from the fracture surfaces of the specimens subjected to low cycle and high cycle fatigue regimes, respectively. It may be recalled that the specimens were loaded in a direction 90° to the fiber axis. The fracture features of the specimen at different magnifications are presented. The location of construction fibers is highlighted.

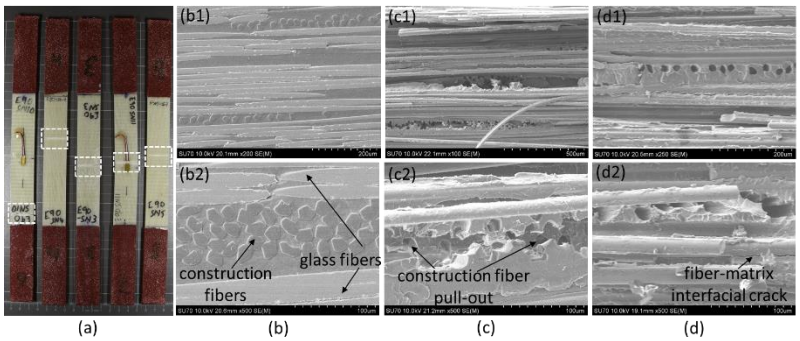

Figure 5: (a) Typical fatigue tested GF/thermoplastic specimens with location of final failure indicated on the specimens, SEM images corresponding to fracture surfaces of the specimens (b) neat specimen, (c) low-cycle fatigue tested specimen, (d) high-cycle fatigue tested specimen.

Figure 5(c) shows localized damage at the regions of the construction fibers with the pull-out of these fibers evident. Pore-like structure caused due to pull-out of the construction fibers during fatigue loading was observed at several locations in the specimen cross-section. Evidence of matrix cracks and fiber-matrix debonding was also seen. Matrix adhesion to debonded and broken fibers was seen pointing to

strong fiber-matrix bonding observed. The pull-out of construction fibers indicates a weaker bonding with the matrix and likely to have served as crack initiation points and damage propagation subsequently. Figure 5(d) shows the fracture surfaces of a high-cycle fatigue tested specimen. Fiber pull-out as in previous case was seen. Fiber-matrix debonding and fiber breakage were observed. The interfacial characteristics indicated a strong fiber-matrix bonding. Matrix cracking leading to separation of fibers was evident. The presence of a thick layers of resin adhering to the fibers was seen at several locations. Overall, the fiber bundles remained intact and their separation was lower as compared to the previous case.

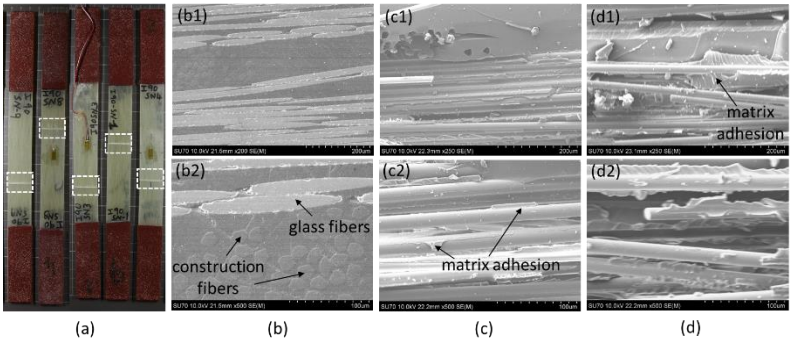

Figure 6: (a) Typical fatigue tested GF/bio-epoxy specimens with location of final failure indicated on the specimens, SEM images corresponding to fracture surfaces of the specimens (b) neat specimen, (c) low-cycle fatigue tested specimen, (d) high-cycle fatigue tested specimen.

Figure 6(a) shows the fatigue tested specimens of GF/bio-epoxy composites with the location of final failure in each specimen highlighted. As in the previous case, the failure occurred in the gauge section of specimens. Localized failure was seen even in this case. Figure 6(b) shows the cross-section of untested specimens. The images indicate the absence of cracks and other damages prior to testing. Presence of construction fibers, grouped on account of resin flow during infusion was observed. Matrix-rich regions were observed from the cross-sectional images of untested specimens. Figure 6(c) shows the fracture surface of the low-cycle fatigue tested specimen. The bio-epoxy matrix was observed to hold the fibers intact and very limited evidence of matrix plastic deformation was observed. The fracture surface was also characterized by matrix-rich regions. Unlike in the case of GF/thermoplastic composites, the construction fibers were seen to be mostly intact with only a few fibers displaced from their position leaving voids in the cross-section. Matrix adhesion to the separated fibers was less pronounced with clean fiber surfaces visible at several locations. Figure 6(d) shows the images taken from the fracture surface of a high-cycle fatigue tested specimen. The fracture surface appeared like that of the low-cycle fatigue specimen. However, matrix deformation was more pronounced and localized damage areas were seen. The construction fibers were mostly intact in their position indicating the presence of a strong matrix. Fiber-matrix adhesion characteristics were similar to that of the low-cycle fatigue specimen. The failure surfaces indicate higher work required for fiber-matrix separation and final failure. This is also supported by the marginally higher fatigue strength values reported in case of GF/thermoplastic composites. Overall, fractography observations support the experimental results.

9 CONCLUSIONS

The fatigue behavior of glass fiber composites fabricated using sustainable polymer matrix systems was investigated in the present work. The objective of the study was to assess the influence of matrix on the fatigue behavior of UD composites loaded transverse to the fiber axis. Based on the results from the study, the following conclusions were drawn

1. The fatigue performance of glass fiber composites was evaluated using two different techniques. Based on the S-N curves, the fatigue performance of both GF/bio-epoxy composites and GF/thermoplastic composites were comparable in both low cycle and high cycle fatigue regimes.

2. From the preliminary test results of thermography analysis, the damage initiation and accumulation in case of GF/thermoplastic composite was found to occur at a faster rate. The stress level determined using this method also indicates that the fatigue performance of glass fiber/Elium composites and glass fiber/Infugreen composites are comparable. Further, the fatigue properties determined from both S-N curve and thermography techniques are in close agreement.
3. Fractography results indicated that matrix damage was more pronounced in case of GF/thermoplastic composites as compared to that of GF/bio-epoxy composites.
4. Pull-out of construction fibers, fiber-matrix debonding, fiber breakage and delamination failure were the mechanisms observed in the composites tested.

ACKNOWLEDGEMENTS

The study presented in this paper was supported by European Union's Horizon 2020 research and innovation programme under grant agreement No. 952966 (FIBREGY Project). The authors like to acknowledge the support received from Mr. Adrian McEvoy, University of Limerick towards mechanical testing. The authors are also thankful to the Bernal Institute and School of Engineering, University of Limerick, Ireland for providing access to test equipment and software for processing the results.

REFERENCES

[1] F. Kanyoko and E. Baker, Uncertainty analysis of the future cost of wind energy on climate change mitigation, *Climatic Change*, **166**, 2021, 10 (doi:10.1007/s10584-021-03105-0).

[2] A. Uihlein and D. Magagna, Wave and tidal current energy – A review of the current state of research beyond technology, *Renewable and Sustainable Energy Reviews*, **58**, 2016, pp. 1070-1081 (doi:10.1016/j.rser.2015.12.284).

[3] S.C. Pryor, R.J. Barthelmie, M.S. Bukovsky, L.R. Leung and K. Sakaguchi, Climate change impacts on wind power generation, *Nature Reviews Earth & Environment*, **1**, 2020, pp. 627–643 (doi:10.1038/s43017-020-0101-7).

[4] A. Azam, A. Ahmed, H. Wang, Y. Wang and Z. Zhang, Knowledge structure and research progress in wind power generation (WPG) from 2005 to 2020 using CiteSpace based scientometric analysis, *Journal of Cleaner Production*, **295,** 2021, 126496 (doi: 10.1016/j.jclepro.2021.126496).

[5] M.D. Esteban, J.J. Diez, J.S. López and V. Negro, Why offshore wind energy?, *Renewable Energy*, **36**, 2011, pp. 444-450 (doi:10.1016/j.renene.2010.07.009).

[6] Z. Jiang, Installation of offshore wind turbines: A technical review, *Renewable and Sustainable Energy Reviews*, ***1*39**, 2021, 110576 (doi:10.1016/j.rser.2020.110576).

[7] K. O'Leary, V. Pakrashi and D. Kelliher, Optimization of composite material tower for offshore wind turbine structures, *Renewable Energy*, **140**, 2019, pp. 928-942 (doi:10.1016/j.rser.2020.110576).

[8] J. Beauson, A. Laurent, D.P. Rudolph and J.P. Jensen, The complex end-of-life of wind turbine blades: A review of the European context, *Renewable and Sustainable Energy Reviews*, **155,** 2022, 111847 (doi:10.1016/j.rser.2021.111847).

[9] M. Rani, P. Choudhary, V. Krishnan and S. Zafar, A review on recycling and reuse methods for carbon fiber/glass fiber composites waste from wind turbine blades, *Composites Part B: Engineering*, **215**, 2021, 108768 (doi:10.1016/j.compositesb.2021.108768).

[10] C.W. Kensche, Fatigue of composites for wind turbines, *International Journal of Fatigue*, **28**, 2006, pp. 1363-1374 (doi:10.1016/j.ijfatigue.2006.02.040).

[11] M. Bakkal, M. Kayihan, A. Timur, Z. Parlar, C.G. Parsiz, A.H. Yucel, I.M. Palabiyik and T. Gulmez, Fatigue behavior and self-heating mechanism of novel glass fiber reinforced

thermoplastic composite, *Advanced Composite Materials, 2023* (doi: 10.1080/09243046.2023.2175764).

[12] C.W. Kensche, Fatigue of composites for wind turbines, *International Journal of Fatigue*, **28**, 2006, pp. 1363-1374 (doi:10.1016/j.ijfatigue.2006.02.040).

[13] S. Liang, P.B. Gning and L. Guillaumat, A comparative study of fatigue behaviour of flax/epoxy and glass/epoxy composites, *Composites Science and Technology*, **72**, 5, 2012, pp. 535-543 (doi:10.1016/j.compscitech.2012.01.011).

[14] A. Makeev, Interlaminar shear fatigue behavior of glass/epoxy and carbon/epoxy composites, *Composites Science and Technology*, **80**, 2013, pp. 93-100 (doi:10.1016/j.compscitech.2013.03.013).

[15] W. Roundi, A.E. Mahi, A.E. Gharad and J.L. Rediere, Experimental and numerical investigation of the effects of stacking sequence and stress ratio on fatigue damage of glass/epoxy composites, *Composites Part B: Engineering*, **109**, 2017, pp. 64-71 (doi:10.1016/j.compositesb.2016.10.044).

[16] Z. Mahboob, Z. Fawaz and H. Bougherara, Fatigue behaviour and damage mechanisms under strain controlled cycling: Comparison of Flax–epoxy and Glass–epoxy composites, *Composites Part A: Applied Science and Manufacturing*, **159**, 2022, 107008 (doi:10.1016/j.compositesa.2022.107008).

[17] D. Palumbo, R.D. Finis, P. G. Demelio and U. Galietti, A new rapid thermographic method to assess the fatigue limit in GFRP composites, *Composites Part B: Engineering*, **103**, 2016, pp. 60-67 (doi:10.1016/j.compositesb.2016.08.007

[18] ISO 13003:2003(E): Fibre-reinforced plastics — Determination of fatigue properties under cyclic loading conditions, 2003.

[19] ISO 527-4, Plastics — Determination of tensile properties — Part 4: Test conditions for isotropic and orthotropic fibre-reinforced plastic composites, 2009.